Molecular Therapy - Methods & Clinical Development 2021 主論文

DOI: https://doi.org/10.1016/j.omtm.2021.03.008

Generation of macrophages with altered viral sensitivity from genome-edited rhesus macaque iPSCs to model human disease

Yoshihiro Iwamoto[1, 2], Yohei Seki[3], Kahoru Taya[1, 4], Masahiro Tanaka[1], Shoichi Iriguchi[1], Yasuyuki Miyake[1], Emi E. Nakayama[4], Tomoyuki Miura[5], Tatsuo Shioda[4], Hirofumi Akari[3,6], Akifumi Takaori-Kondo[2], and Shin Kaneko[1,7]

1. Shin Kaneko Laboratory, Department of Cell Growth and Development, Center for iPS Cell Research and Application(CiRA), Kyoto University, Japan

2. Department of Hematology and Oncology, Graduate School of Medicine, Kyoto University, Japan.

3. Center for Human Evolution Modeling Research, Primate Research Institute, Kyoto

University,, Japan.

4. Research Institute for Microbial Diseases, Osaka University, Japan

5. Laboratory of Primate Model, Research Center for Infectious Diseases, Institute for Frontier Life and Medical Science, Kyoto University, Japan

6. Laboratory of Infectious Disease Model, Institute for Frontier Life and Medical Sciences, Kyoto University, Japan

7. Correspondence should be addressed to Shin Kaneko (kaneko.shin@cira.kyoto-u.ac.jp)

The study was performed at the Center for iPS Cell Research and Application (CiRA), Kyoto University, 53 Shogoin Kawahara-cho, Sakyo-ku, Kyoto, Japan

Correspondence: Shin Kaneko Laboratory, Department of Cell Growth and Differentiation, Center for iPS Cell Research and Application (CiRA), Kyoto University, 53 Shogoin Kawahara-cho, Sakyo-ku, Kyoto, Japan

E-mail: kaneko.shin@cira.kyoto-u.ac.jp

Short title : Macrophages from genome edited rhesus macaque iPSC

Abstract

Because of their close biological similarity to humans, non-human primate (NHP) models are very useful for the development of induced pluripotent stem cell (iPSC)-based cell and regenerative organ transplantation therapies. However, knowledge on the establishment, differentiation and genetic modification of NHP-iPSCs, especially rhesus macaque iPSCs, is limited. We succeeded in establishing iPSCs from the peripheral blood of rhesus macaques (Rh-iPSCs) by combining the Yamanaka reprograming factors and two inhibitors (GSK-3 inhibitor (CHIR 99021) and MEK1/2 inhibitor (PD0325901)) and differentiated the cells into functional macrophages through hematopoietic progenitor cells. To confirm feasibility of the Rh-iPSC-derived macrophages as a platform for bioassays to model diseases, we knocked out *TRIM5* gene in Rh-iPSCs by CRISPR/Cas9, which is a species-specific HIV resistance factor. *TRIM5* KO iPSCs had the same differentiation potential to macrophages as Rh-iPSCs, but the differentiated macrophages showed a gain of sensitivity to HIV infection in vitro. Our reprogramming, gene editing, and differentiation protocols used to obtain Rh-iPSC-derived macrophages can be applied to other gene mutations, expanding the number of NHP gene therapy models.

Introduction

Induced pluripotent stem cells (iPSCs) are expected to have many clinical applications in regenerative medicine because of their unlimited self-renewal ability and potential to differentiate into any type of cell or tissue [1]. Several groups including ours are preparing iPSCs from mature blood cells and differentiating them into hematopoietic stem cells, lymphocytes, and macrophages with the aim of treating a wide variety of diseases including cancer and viral infections [2-4]. In addition, iPSCs are an ideal platform to perform genetic engineering such as genome editing technology and viral gene transduction, because the genomic integrity of the edited cells can be thoroughly assessed due to their high cloning efficiency. The utility of iPSC-based regenerative medicine is further augmented when combined with gene engineering. In fact, the possibility of HIV treatment with macrophages derived from iPSCs transfected with shRNA targeting the HIV promotor has been reported[5]. Functional immune cells induced by genome editing at the iPSC stage have also been reported [6.7.8].

The in vivo evaluation of the efficacy and safety, including tumorgenicity and immunogenicity in preclinical models, is essential for the clinical application of iPSC products, but most reports have evaluated safety in immunodeficient mice only. Non-human primate (NHP) models are preferred preclinical animal models because of the

73 stronger similarities between NHPs and humans compared with mice and humans.
74 Accordingly, NHP-iPSCs for the treatment of retinal disease, Parkinson's disease, heart
75 disease and hereditary bone disease have been reported, as have their use for the
76 production of myocardial and bone cells and myocardial allogeneic transplantation[9-13].
77 NHPs are phylogenetically very close to humans in their size, lifespan, and immune
78 system [12,14.15]. Additionally, the adaptive and innate immune responses to antigens in
79 NHPs are very similar to those in humans. Among NHPs, rhesus macaques (Rh) are
80 suitable for immunological analysis, including studies investigating viral infections and
81 allogeneic transplantations, because their major histocompatibility complexes (MHCs)
82 have been analyzed in detail[16-18]. Accordingly, iPSCs of reprogrammed Rh cells (Rh-
83 iPSCs) and Rh-iPSC-derived immune cells may be useful tools for studying immune
84 responses in vitro and in vivo. In addition, Rh-iPSCs resemble human iPSCs in terms of
85 morphology, marker expression, and growth factor dependency [19].
86 In this study, as a proof of concept for the gain or loss of function in cells differentiated
87 from gene-edited Rh-iPSCs, we knocked out *TRIM5* in Rh-iPSCs by the CRISPR/Cas9
88 system. TRIM5α is known to be a species-specific HIV resistance factor in Rh [20-22]. It is
89 also reported that the HIV resistance of Rh CD4 lymphocytes is lost in vitro by the
90 knockout (KO) of TRIM5α in peripheral blood CD4 lymphocytes with TALEN [23]. We

differentiated wild-type and *TRIM5* KO Rh-iPSCs into hematopoietic progenitor cells (HPCs) and macrophages and compared their functions, finding the KO iPSC products showed a gain of sensitivity to HIV.

The reprogramming, differentiation, and gene editing techniques for Rh cells presented in this paper will contribute to the development of preclinical NHP models for HIV infection using CCR5 KO HPC transplantation[24,25] or allogeneic organ transplantations derived from HLA-KO iPSCs[26].

Results

1 Generation of Rh-iPSCs from Rh peripheral blood mononuclear cells

Rh-iPSCs have been established from fibroblasts, bone marrow stromal cells, and CD34(+) hematopoietic stem/progenitor cells (HSPCs) [11,12,19,27,28,29], but not from peripheral blood mononuclear cells (PBMCs), which has become mainstream from the viewpoints of invasiveness, sterility, and ease of collection for generation of human iPSCs (ref) [2,3,7].

In this study, following the reprogramming protocol for human iPSCs, we transfected Rh PBMCs with a Sendai virus (SeV) vector encoding the Yamanaka factors (OCT3/4, SOX2, KLF4, c-MYC) [30] to establish Rh-iPSCs. Notably, no colonies were observed if medium including bFGF, which is typically used to reprogram Rh fibroblasts, was used for the reprogramming. Therefore, we applied 2i medium, which adds GSK-3 inhibitor (CHIR 99021) and MEK1/2 inhibitor (PD0325901) [31] to the original iPSC maintenance medium. In this case, dome-shaped colonies were observed about 25-30 days after the transfection (Figure 1a,b). The reprogramming was confirmed using cells from three Rh (animal ID : R1863, R1887, R1889)(Figure 1c). Residual SeV was detected in one Rh-iPSC clone prepared from one individual, but not in any of the remaining clones (Figure 1d). We confirmed that the Rh-iPSCs expressed Nanog, KLF4, POU5F1, SOX2, and c-Myc by

RT-PCR and SSEA4, a marker of undifferentiated iPSCs, by FACS (Figure1 e,f). We also verified pluripotency by detecting teratoma that could differentiate into the three germ layers (Figure 1g). Finally, Rh-iPSCs could be maintained for more than 50 passages with normal karyotype (Figure 1h).

2 Differentiation of Rh-iPSCs into HPCs

By applying a reported human iPSC differentiation protocol[2,5] (Figure 2a), we could differentiate all Rh-iPSC clones into CD34(+) cells (Figure 2b,c). To improve the efficiency of the CD34(+) cell induction, we added BMP4, which is reported to promote mesoderm differentiation[32-34], on day 0 of the protocol (Figure 2d). Table 1 shows a summary of the number of CD34(+) cells. A colony-forming unit assay (CFU assay) was performed to evaluate if the CD34(+) cells represent HPCs. We confirmed colonies containing CFU-M (macrophage), CFU-GM (granulocyte/macrophage), CFU-G (granulocyte) and CFU-E (erythroid) at an efficiency of about 0.6% (Figure 2e). These results indicate that CD34(+) cells differentiated from Rh-iPSCs were multipotential HPCs.

3 Differentiation of Rh-iPSCs into macrophages

145 Next, we induced Rh-iPSC-derived HPCs into macrophages, which are target cells for
146 HIV/SIV (simian immunodeficient virus), using the human iPSC differentiation method
147 established by our group[5]. After the HPCs were co-cultured with C3H10T1/2 feeder for
148 10 days in the presence of M-CSF and GM-CSF, adherent cells were seeded on a low-
149 adsorption plate and further cultured for about 10 days to differentiate into macrophages
150 (Figure 3a). Starting with confluent Rh-iPSCs in a 6-cm dish, about 1-2 × 10^7
151 macrophages could be obtained on days 34. After day 34, the macrophages showed no
152 obvious growth. FACS analysis showed that the induced macrophages were
153 CD11b(+)/CD14(+)/CD68(+)/CD86(+)/CD163(-). They also expressed CCR5, which is
154 a co-receptor for HIV/SIV (Figure 3b, S1a). The phenotypes of the Rh-iPSC-derived
155 macrophages resembled those of monocyte-derived macrophages (Figure S1b). We
156 confirmed phagocytosis by the induced macrophages after one hour co-culturing with
157 Alexa Flour594-conjugated Escherichia coli bioparticles (Figure 3c). Additionally,
158 macrophages stimulated with LPS produced the inflammatory cytokines TNF and IL-6
159 (Figure 3d).
160 We also stimulated the induced macrophages by SIV infection. Macrophage tropic
161 SIVmac316 and T cell tropic SIVmac239 were co-cultured with the induced macrophages,
162 and p27 protein was measured by ELISA on days 1, 4, and 7. The production of p27

protein was observed in the SIVmac316 co-culture but not the SIVmac239 co-culture (Figure 3e). These results suggest that functional macrophages with SIV sensitivity can be differentiated from Rh-iPSCs by our protocol.

4 Generation of TRIM5 KO Rh-iPSCs by CRISPR/Cas9

We next used CRISPR/Cas9 to genome edit the Rh-iPSCs. TRIM5α is an HIV resistance factor in Rh. It has a PRYSPRY region at its C-terminal that is connected via a long link to the N-terminal, which includes three motifs: a RING domain, B-box2 domain, and coiled-coil domain. We knocked out TRIM5α using the CRISPR/Cas9 system in Rh-iPSCs. Candidate sequences for the sgRNA were selected using CRISPOR (http://crispor.tefor.net/crispor.py). The target sequence is shown in Figure 4a. We transfected sgRNA and Cas9 protein into Rh-iPSCs by electroporation and picked up 24 colonies manually without drug selection. An analysis of the genomic sequences of *TRIM5* in the 24 clones revealed mutations in 7 clones, with 3 of them showing homozygous mutations in *TRIM5* (Figure 4b). These clones had an in-frame mutation in a single allele. By randomly selecting one clone from the heterozygous clones and performing additional genome editing, we were able to create TRIM5αKO Rh-iPSCs, in which the stop codon due to a frameshift mutation was confirmed (Figure 4c). The

PRYSPRY region is considered to be important for controlling HIV infection[21]. Because the stop codon existed at exon3 in TRIM5αKO Rh-iPSCs, the PRYSPRY region downstream of exon3 was not translated. Thus, we expected TRIM5αKO Rh-iPSCs to have lost their resistance to HIV infection. When the expression of TRIM5αKO Rh-iPSC mRNA was measured by qPCR, the expression level of TRIM5α was decreased in all three strains, which is considered to be caused by nonsense mutation-dependent mRNA degradation (NMD)[35,36] (Figure 4d). Next, we evaluated the differentiation potential of TRIM5αKO Rh-iPSCs in reference to parental Rh-iPSCs. Parental Rh-iPSCs and TRIM5αKO Rh-iPSCs had equivalent efficiencies for differentiating into CD34(+) cells and macrophages (Figure 4e,f). The expression of CD86 were different between macrophages differentiated from parental and TRIM5αKO. One report found that primate dendritic cells (DCs) lacking efficient TRIM5α-mediated retroviral restriction upregulate CD86 expression[37]. We hypothesize that the expression of CD86 was increased in TRIM5αKO macrophages by the same mechanism. Additionally, we confirmed no potential off-target sites in the TRIM5αKO Rh-iPSC clones for the gRNAs, as identified by CRISPOR software and Sanger sequencing (Table 2). From these results, we confirmed the genome editing of Rh-iPSCs did not compromise the differentiation potential.

199

200 ***5 Deletion of TRIM5a enables HIV-1 virus infection***

201 In order to confirm that TRIM5α was functionally knocked out in TRIM5αKO Rh-iPSCs,
202 we infected the induced macrophages with HIV (VSV-G-pseudotyped lentivirus vector
203 expressing luciferase (NL43-Luci/VSV-G)[38]). HIV (NL43-Luci/VSV-G) was co-cultured
204 with macrophages differentiated from TRIM5αKO Rh-iPSCs and parental Rh-iPSCs.
205 Luminescence was increased in macrophages differentiated from TRIM5αKO Rh-iPSCs
206 compared with parental Rh-iPSCs on all days observed (2, 3, and 4), suggesting that the
207 TRIM5αKO Rh-iPSC-derived macrophages lost their resistance to the early stage of HIV
208 infection (Figure 5a). To determine if the HIV infection was caused by the loss of TRIM5α,
209 which degrades HIV at the reverse transcription stage, we tested a reverse transcriptase
210 inhibitor (Nevirapine: NVP), finding it suppressed the HIV infection of TRIM5αKO Rh-
211 iPSC-derived macrophages (Figure 5b). From these results, we showed that it is possible
212 to control the HIV resistance of Rh-iPSC-derived macrophages by gene editing *TRIM5*.

213

214

215

216

Discussion

As the first step in creating an NHP model for evaluating the efficacy and safety of genome edited iPSC-derived cells, we established a method to generate iPSCs from Rh PBMCs, induce their differentiation to HPCs/macrophages, and edit target genes using the CRISPR/Cas9 system. As a proof of concept, we showed that macrophages from iPSCs in which TRIM5α was deleted lost their resistance in the early stage of HIV infection.

By adding GSK-3 inhibitor (CHIR 99021) and MEK1/2 inhibitor (PD0325901) (i.e. '2i') to the iPSC medium, we could generate iPSCs from Rh PBMCs that can be collected aseptically and relatively easily. 2i was originally reported to maintain mouse embryonic stem cells (ESCs)[31], but has since been applied to maintain iPSCs from various species[39,40,41]. Interestingly, Rh-iPSCs have been established and maintained without 2i, but from fibroblasts, bone marrow stromal cells, and CD34(+) HPCs, all of which are shallowly differentiated cells. We found 2i was required for reprogramming more differentiated cells such as PBMCs.

In this study, we show that BMP4 improved the efficiency to induce HPCs from Rh-iPSCs. This effect is consistent with human iPSCs[33] and pigtail macaque iPSCs[34]. In order to acquire a massive amount of HPCs for transplantation experiments, it is essential to

235 optimize the differentiation induction conditions. With our culture method, we could
236 generate about 1-2 × 10^7 HPCs from rh-iPSCs cultivated on a 6-cm dish (Table 1). This
237 massive amount is expected to achieve long-term engraftment by autologous or allogenic
238 transplantation when supported by the appropriate environment such as niche and
239 cytokines.
240 Macrophages are immune cells that play an important role in eliminating pathogens and
241 dying cells. They also express CD4 and CCR5, which are HIV/SIV receptors, and act as
242 HIV/SIV virus reservoirs. The possibility of treating HIV infection with macrophages
243 regenerated from human iPSCs transfected with shRNA targeting HIV-1 promotor or with
244 CCR5 KO has been reported[5,8]. By using genome-edited Rh-iPSC-derived macrophages,
245 the findings of human iPSC-derived macrophages can be verified with an NHP model,
246 advancing research on viral infections including HIV/SIV and corresponding treatments.
247 Following this approach, we confirmed that HIV could infect TRIM5αKO iPSC-derived
248 macrophages, not CD4(+) T cells. A protocol to induce CD4(+) T cells is for future work.
249 Gene transfer by homology directed repair using the CRISPR/Cas9 system for Rh-iPSCs
250 has been reported[29], but the present study is the first to report functional loss due to non-
251 homologous end joining. We found poor efficiency for the genome editing of Rh-iPSCs
252 by the conventional CRISPR/Cas9 system using plasmid DNA (Table S1). Furthermore,

253 the technique was technically difficult. In contrast, the ribonucleoprotein method we used
254 raises the efficiency while simplifying the sgRNA synthesis.
255 Finally, our genome editing of TRIM5 in Rh-iPSCs is a proof of concept for other target
256 genes. One possibility is a gene therapy model for HIV created by transplanting HPCs
257 derived from CCR5 KO Rh-iPSCs. Furthermore, the present method will contribute to
258 preclinical models such as the development of NHP models for the allogeneic
259 transplantation of HLA-KO iPSC-derived cells/tissues.
260
261
262
263
264
265
266
267
268
269
270

Material & Methods

Animal Use

All animals used in this study were housed and handled in accordance with protocols approved by Primate Research Institute, Kyoto University (2016-C-5).

Generation of Rh-iPSCs from rhesus macaque PBMCs

Rh-iPSCs were generated from rhesus macaque PBMCs. PBMCs were stimulated by α-CD2/3/28-coated beads (Miltenyi Biotech Cat no: 130-092-919). After 4 days, the PBMCs were transduced with Sendai virus (SeV) vectors harboring OCT3/4, KLF2, SOX2, c-MYC[30] and SV40 large T antigen, and then seeded onto inactivated mouse embryonic feeder cells (MEFs). The cultured medium was gradually replaced with Rhesus iPSC medium (Dulbecco's modified Eagle's medium/F12 HAM (SIGMA) supplemented with 20% knockout serum replacer (Thermo Fischer Scientific), 1% L-Glutamine–Penicillin–Streptomycin solution (SIGMA), 1% nonessential amino acids (Thermo Fischer Scientific), 10 mM 2-mercaptoethanol, and 5 ng/ml bFGF (Wako), in addition to 3 μM GSK-3 inhibitor CHIR 99021 (Tocris) and 2 μM MEK1/2 inhibitor PD0325901 (Wako). The established iPSC clones were transfected with small interfering RNA L527[30] using Lipofectamine RNAi Max (Invitrogen) to remove the SeV vectors

289 from the cytoplasm.

290

291 **Rh-iPSC maintenance and passage**

292 Rh-iPSC medium was replaced with 1 ml per 60-mm dish of dissociation solution
293 consisting of 20 ml 2.5% Trypsin (Invitrogen), 40 ml Knockout Serum Replacement
294 (Invitrogen), and 2 ml 100 mM $CaCl_2$ to 138 ml D-PBS (-) (Nacalai; Japan), and the cells
295 were then incubated at 37℃ in a CO_2 incubator for 5 min. After the incubation, MEFs
296 and dissociation solution were removed, and 1 ml of Rh-iPSC culture medium was added.
297 The colonies were broken up into small cell clumps by pipetting. About one-fifth of the
298 cell suspension was transferred to a new MEF dish, although the split ratio may require
299 adjustment depending on the iPSC line. The medium was replaced with fresh medium
300 every day.

301

302 **Teratoma formation**

303 Rh-iPSCs at a confluency of 70-80% were harvested by using Trypsin EDTA, and 2 ×
304 10^6 iPSCs were suspended with 100 µl of Matrigel and 100 µl of cold PBS. Rh-iPSCs
305 were injected subcutaneously into 6-week-old female NOD.Cg-*Prkdc*^{scid} *Il2rg*^{tm1Wjl}/SzJ
306 (NSG) mice, and 8-10 weeks later, teratomas were dissected and fixed in formaldehyde.

Differentiation of Rh-iPSCs into HPCs

To induce hematopoietic differentiation from Rh-iPSCs, we slightly modified a previously described human iPSC method[2]. In brief, small clumps (<100 cells) of Rh-iPSCs maintained on MEFs were collected and co-cultured on C3H10T1/2 feeder cells in EB medium (Iscove's modified Dulbecco's medium (SIGMA) containing of 20% FBS, 1% L-Glutamine–Penicillin–Streptomycin solution (SIGMA), 100x Insulin-Transferrin-Selenium solution (Thermo Fisher Scientific), 450 μM monothioglycerol (Nacalai), 50 μg/ml Ascorbic acid 2-phosphate (Nacalai)), in addition to 20 ng/ml VEGF (R&D systems). On day 0, 20 ng/ml BMP4 (R&D Systems), and on days 7,10, and 12, 30 ng/ml SCF (R&D systems) and 10 ng/ml FLT-3L (Peprotech) were added to EB medium. Hematopoietic cells generated in iPSC sacs were collected on day 14.

Differentiation of Rh-iPSCs into macrophages

On day 14, the collected hematopoietic cells were transferred onto newly prepared C3H10T1/2 feeder cells in EB medium containing 50 ng/ml M-CSF (Peprotech) and 25 ng/ml GM-CSF (Peprotech). On day 24, after the floating and loosely adherent cells were removed, firmly adherent cells were collected and transferred to low-attachment six-well

culture plates (Corning Costar Ultra-Low attachment multiwell culture plates; Sigma-Aldrich) in EB medium containing GM-CSF (50 ng/ml) and M-CSF (25 ng/ml) and differentiated to macrophages after about 10 more days.

Flow cytometry

Stained cell samples were analyzed using an LSR fortessa (BD Biosciences), and the data were processed using FlowJo (Tree Star). The following antibodies were used: APC-CD34 (clone 563; BD Bioscience), BV510-CD45 (clone D058-1283; BD Bioscience), BV421-CD4 (clone OKT4; BioLegend), APC-cy7-CD11b (clone M1/70; BioLegend), PE/Cy7-CD14 (clone M5E2; BioLegend), Alexa Flour 648-CD68 (clone KP1; Santa cruz), PacificBlue-CD86 (clone IT2.2; BioLegend), PerCPcy5.5-CD163 (clone GHI/61; BioLegend), APC-CCR5 (clone 3A9; BD Bioscience), and PE-SSEA4 (clone FAB1435P; R&D).

Colony forming unit assay

CD34(+) cells were sorted using a FACS AriaIIflow cytometer (BD Biosciences) from day 14 of the hematopoietic differentiation culturing. A total of 5000 cells per 35-mm dish were seeded in Methocult (H4435; STEMCELL TECHNOLOGIES) containing 1%

L-Glutamine–Penicillin–Streptomycin solution (SIGMA) and cultured for 14 days in a 37℃ incubator. Representative colonies were picked up and analyzed by microscopic morphology after Giemsa staining.

Analysis of phagocytosis function of macrophages differentiated from Rh-iPSCs

Macrophages were co-cultured with Alexa Flour594-conjugated Escherichia coli Bioparticles (Thermo Fisher) for 1 hour, washed three times with PBS, and observed by an IX71 inverted microscope (Olympus).

Analysis of cytokine production of macrophages differentiated from Rh-iPSCs

Macrophages were cultured in 96-well plates (5×10^4 cells/200 μl EB medium containing GM-CSF (50 ng/mL) and M-CSF (25 ng/mL)) in the presence of LPS (0, 1, or 10 ng/ml). After 24 h culture, the supernatant was collected, and the concentrations of TNF and IL-6 were measured by using a CBA Human Inflammatory Cytokine Kit (BD, Cat.No.551811).

***TRIM5* targeted sgRNA construction**

Candidate sequences targeting rhesus *TRIM5* were selected using CRISPOR

(http://crispor.tefor.net/crispor.py). The designed gRNAs were synthesized by *in vitro* transcription using a MEGAshortscript kit (Thermo Fisher Scientific, Cat. No. AM1354) according to the instruction manual.

CRISPR-Cas9 genome editing experiments

Transfection was performed by using MaxCyte STx (MaxCyte). 1.5×10^6 iPSCs were transfected with an RNP (ribonucleoprotein) complex consisting of 10 μg recombinant Cas9 (IDT, Cat. No. 1074181) and 2.5 μg of IVT gRNA in 50 μl hyclone electroporation buffer. After electroporation, the cells were transferred to a MEF-coated plate in Rh-iPSC medium containing ROCK inhibitor Y-27632 for 3 days and then passaged to a new MEF-coated plate. Without drug selection, single colonies were manually picked up and cloned.

SIV infection and viral quantification

A total of 1 $x10^5$ differentiated macrophages were infected with SIV mac 316 or SIV mac 239 for 2 hours at 37 ℃, washed 2 times with PBS to remove the free virus, and cultured for 10 days. The culture supernatants were collected at days 1, 4, and 7 and measured for p27 antigen by ELISA according to the manufacturer's instruction (Zeptmetrix, CatNo:

0801201).

HIV-1 infection and luciferase assay

For VSV-G-pseudotyped lentivirus vector expressing luciferase (NL43- Luci/VSV-G)[38] preparation, human embryonic kidney cells (293T cells) were transfected with 15 mg of pNL4-3-Luc-R-E- plasmid and 5 mg of VSV-G-encoding plasmid, and viruses were harvested 48 h later. Differentiated macrophages were infected with NL43- Luci/VSV-G for 2 hours in a 37℃ incubator, washed 2 times with PBS to remove the free virus, and cultured for 4 days in the presence or absence of 2 μM of an anti-HIV drug, Nevirapine (SIGMA). At days 2, 3, and 4, luciferase activity in the cell lysate was measured by using a Luciferase Assay System (Promega, Cat.No.E1500) and Lumat LB 9507 (Berthold).

Statistics

GraphPad PRISM (GraphPad Software) was used for all statistical analyses. Paired or unpaired Student's t-tests or two-way ANOVA with Tukey's multiple comparison test were performed to assess the statistical significance of differences between groups.

Author Contribution

Y.I., Y.S., E.N., T.S., H.A., and S.K. conceived and designed the experiments. Y.I., Y.S., K.T., and M.T. performed the experiments or analyzed the data. T.S., H.A., A. T-K., and S.K. drafted and edited the manuscript. S.I., Y.M., E.N, and T.M. provided technical support. T.S. provided critical materials, including HIV virus. All authors reviewed the manuscript.

Disclosure/ Conflicts of Interest

Shin Kaneko is a founder, shareholder, and chief scientific officer at Thyas Co., Ltd., and received research funding from Takeda Pharmaceutical Co. Ltd., Kirin Holdings Co., Ltd., Astellas Co. Ltd, Terumo Co., Ltd., Tosoh Co. Ltd., and Thyas Co., Ltd.

Acknowledgments

This research was supported by AMED under Grant Number 20fk0410033h0001, the Cooperative Research Program of the Primate Research Institute, Kyoto University, and the Cooperative Research Program (Joint Usage/Research Center Program) of the Institute for Frontier Life and Medical Sciences, Kyoto University.

We thank Huaigeng Xu, Tatsuki Ueda (Kyoto University), and Peter Gee (MaxCyte) for

giving critical advice on the genome editing technique; Eri Imai, Sanae Kamibayashi, Kohei Ohara, Tomoko Ishii, Kaede Makino and Munehiro Yoshida (Kyoto University) for technical assistance; Mahito Nakanishi (National Institute of Advanced Industrial Science and Technology) for providing the SeV; and Peter Karagiannis (Kyoto University) for editing the manuscript.

References

1. Takahashi, K., Tanabe, K., Ohnuki, M., Narita, M., Ichisaka, T., Tomoda, K., and Yamanaka, S. (2007). Induction of pluripotent stem cells from adult human fibroblasts by defined factors. Cell 131：861－872.
2. Nishimura, T., Kaneko, S., Kawana-Tachikawa, A., Tajima, Y., Goto, H., Zhu, D., Nakayama-Hosoya, K., Iriguchi, S., Uemura, Y., Shimizu, T., et al. (2013). Generation of rejuvenated antigen-specific T cells by reprogramming to pluripotency and redifferentiation. Cell Stem Cell 12, 114–126.
3. Vizcardo, R., Masuda, K., Yamada, D., Ikawa, T., Shimizu, K., Fujii, S., Koseki, H., and Kawamoto, H. (2013). Regeneration of human tumor antigen-specific T cells from iPSCs derived from mature CD8(+) T cells. Cell Stem Cell 12, 31–36.
4. Ando, M., Nishimura, T., Yamazaki, S., Yamaguchi, T., Kawana-Tachikawa, A., Hayama, T., Nakauchi, Y., Ando, Jun., Ota, Y., Takahashi, S., et al. (2015) A safeguard system for induced pluripotent stem cell-derived rejuvenated T cell therapy. Stem Cell Reports 5:597–608
5. Higaki, K., Hirao, M., Kawana-Tachikawa, A., Iriguchi, S., Kumagai, A., Ueda, N., Bo, W., Kamibayashi, S. Watanabe, A., Nakauchi, H., et al. (2018). Generation of HIV-resistant macrophages from IPSCs by using transcriptional gene silencing and

promoter-targeted RNA. Mol Ther Nucleic Acids, 12 :793-804

6. Xu, H., Bo, W., Ono, M., Kagita, A., Fujii, K., Sasakawa, N., Ueda, T., Peter, G., Nishikawa, M., Nomura, M., et al. (2019). Targeted Disruption of HLA Genes via CRISPR-Cas9 Generates iPSCs with Enhanced Immune Compatibility. Cell Stem Cell 24, 566-578

7. Minagawa, A., Yoshikawa, T., Yasukawa, M., Hotta, A., Kunitomo, M., Iriguchi, S., Takiguchi, M., Kassai, Y., Imai, E., Yasui, Y., et al. (2018) Enhancing T Cell Receptor Stability in Rejuvenated iPSC-Derived T Cells Improves Their Use in Cancer Immunotherapy. Cell Stem Cell 23(6):850-858.e4.

8. Kang, H., Minder, P., Park, M. A., Walatta-Tseyon, M., Torbett, B. E., and Slukvin, I. I. (2015). CCR5 Disruption in Induced Pluripotent Stem Cells Using CRISPR/Cas9 Provides Selective Resistance of Immune Cells to CCR5-tropic HIV-1 Virus. Mol Ther Nucleic Acids, 4 :e268

9. Kamao, H., Mandai, M., Okamoto, S., Sakai, N., Suga, A., Sugita, S., Kiryu, J., and Takahashi, M. (2014). Characterization of Human Induced Pluripotent Stem Cell-Derived Retinal Pigment Epithelium Cell Sheets Aiming for Clinical Application. Stem Cell Reports 2(2):205-18.

10. Hallett, PJ, Deleidi, M, Astradsson, A, Smith, GA, Cooper, O, Osborn, TM., Sundberg,

469 M., Moore, M. A., Perez-Torres, E., Brownell, Anna-Liisa., et al. (2015). Successful
470 function of autologous iPSC-derived dopamine neurons following transplantation in
471 a non-human primate model of Parkinson's disease. Cell Stem Cell 16: 269–274.
472 11. Lin, Y., Liu, H., Klein, M., Ostrominski, J., Hong, S. G., Yada, R. C., Chen, G.,
473 Navarengom, K., Schwartzbeck, R. San, H., et al. (2018). Efcient diferentiation of
474 cardiomyocytes and generation of calcium-sensor reporter lines from nonhuman
475 primate iPSCs. Sci Rep Apr 12;8(1):5907
476 12. Hong, S. G., Winkler, T., Wu, C., Guo, V., Pittaluga, S., Nicolae, A., Donahue, R. E.,
477 Metzger, M. E., Price, S. D., Uchida, N., et al. (2014). Path to the Clinic: Assessment
478 of iPSC-Based Cell Therapies In Vivo in a Nonhuman Primate Model. Cell Rep 7,
479 1298-1309
480 13. Shiba, Y., Gomibuchi, T., Seto, T., Wada, Y., Ichimura, H., Tanaka, Y., Ogasawara, T.,
481 Okada, K., Shiba, N., Sakamoto, K., et al. (2016). Allogeneic transplantation of iPS
482 cell-derived cardiomyocytes regenerates primate hearts. Nature 538(7625):388-391
483 14. Hong, S. G., Lin, Y., Dunbar, C.E., and Zou, J. (2016). The Role of Nonhuman Primate
484 Animal Models in the Clinical Development of Pluripotent Stem Cell Therapies. Mol
485 Ther 24(7):1165-9.
486 15. Jacob, D. E., Scott, W. W., and Jason, M. B. (2018). Nonhuman primate models of

487 human viral infections. Nat Rev Immunol 18(6), 390-404

488 16. de Groot, N., Doxiadis, G. G., Otting, N., de Vos-Rouweler, A. J., and Bontrop, R. E.

489 (2014). Differential recombination dynamics within the MHC of macaque species.

490 Immunogenetics 66, 535–544

491 17. Doxiadis, G. G., de Groot, N., Otting, N., de Vos-Rouweler, A. J., Bolijn, M. J.,

492 Heijimans, C. M., de Groot, N., Van der Wiel, M., Remarque, E. J., Vangenot, C., et

493 al. (2013). Haplotype diversity generated by ancient recombination-like events in the

494 MHC of Indian rhesus macaques. Immunogenetics 65,569–584

495 18. Hansen, S. G., Wu, H. L., Burwitz, B.J., Hughes, C. M., Hammond, K. B., Ventura,

496 A.B, Reed, S. R., Gilbride, R. M., Ainslie, E., Morrow, D. W., et al. (2016). Broadly

497 targeted CD8+ T cell responses restricted by major histocompatibility complex E.

498 Science 351, 714–720

499 19. Liu, H., Zhu, F., Yong, J., Zhang, P., Hou, P., Li, H., Jiang, W.,Cai, J., Liu, M., Cui,

500 K., et al. (2008). Generation of induced pluripotent stem cells from adult rhesus

501 monkey fibroblasts. Cell Stem Cell. 3: 587-590

502 20. Stremlau, M., Owens, C.M., Perron, M. J., Kiessling, M., Autissier, P., and Sodrosk,

503 J. (2004). The cytoplasmic body component TRIM5a restricts HIV-1 infectionin Old

504 World monkeys. Nature 427(6977):848-53

505 21. Nakayama, E. E., Miyoshi, H., Nagai, Y., and Shioda, T. (2005). A specific region of
506 37 amino acid residues in the SPRY (B30.2) domain of African green monkey
507 TRIM5alpha determines species-specific restriction of simian immunodeficiency
508 virus SIVmac infection. J. Virol. 79, 8870–8877.
509 22. Ganser- Pornillos, B. K., and Pornillos, O. (2019) Restriction of HIV-1 and other
510 retroviruses by TRIM5. Nat Rev Microbiol (9):546-556.
511 23. Wang, X., Yu, Q., Yuan, Y., Teng, Z., Li, D., and Zeng, Y. (2017). Targeting the rhesus
512 macaque TRIM5a gene to enhance the susceptibility of CD4+ T cells to HIV-1
513 infection. Arch Virol 162(3):793–798
514 24. Hütter, G., Nowak, D., Mossner, M., Ganepola, S., Müssig, A., Allers, K., Scheneider,
515 T., Hofmann, J., Kücherer, C., Blau, O., Blau, I. W., et al. (2009). Long-Term Control
516 of HIV by CCR5 Delta32/ Delta32 Stem-Cell Transplantation. N Engl J Med
517 360(7):692-8.
518 25. Gupta, R. K., Abdul-Jawad, S., McCoy, L. E., Mok, H. P., Peppa, D., Salgado, M.,
519 Martinez-Picado, J., Nijhuis, M., Wensing, A. M. J., Lee, H., et al. (2019). HIV-1
520 remission following CCR5Δ32/Δ32 haematopoietic stem-cell transplantation. Nature
521 568(7751):244-248.
522 26. Riolobos, L., Hirata, R. K., Turtle, C. J., Wang, P-R., Gornalusse, G. G., Zavajlevski,

523 M., Riddell, S. S., and Russel, D. W. (2013). HLA engineering of human pluripotent
524 stem cells. Mol Ther (6):1232-41.
525 27. Fang, R., Liu, K., Zhao, Y., Li, H., Zhu, D., Du, Y., Xiang, C., Li, X., Liu, H., Miao,
526 Z., et al. (2014). Generation of Naive Induced Pluripotent Stem Cells from Rhesus
527 Monkey Fibroblasts. Cell Stem Cell 15(4):488-497.
528 28. D'souza, S. S., Maufort, J., Kumar, A., Zhang, J., Smuga-Otto, K., Thomason, J. A.,
529 and Slukvin, I. I. (2016). GSK3β Inhibition Promotes Efficient Myeloid and
530 Lymphoid Hematopoiesis from Non-human Primate-Induced Pluripotent Stem Cells.
531 Stem Cell Reports 6(2):243-56.
532 29. Hong, S. G., Yada, R. C., Choi, K., Carpentier, A., Liang, T. J., Merling, R. K.,
533 Sweeney, C. L., Malech, H. L., Jung, M., Corat, M.A.F., et al. (2017). Rhesus iPSC
534 Safe Harbor Gene-Editing Platform for Stable Expression of Transgenes in
535 Differentiated Cells of All Germ Layers. Mol Ther 25(1):44-53.
536 30. Nishimura, K., Sano, M., Ohtaka, M., Furuta, B., Umemura, Y., Nakajima, Y., Ikehara,
537 Y., Kobayashi, T., Segawa, H., Takayasu, S., et al. (2011). Development of defective
538 and persistent Sendai virus vector: a unique gene delivery/expression system ideal for
539 cell reprogramming. J Biol Chem 286(6):4760-7
540 31. Ying, Qi-L., Wray, Jason., Nicholas, J., Batlle-Morera, L., Doble, B., Woodgett, J.,

541 Cohen, P., and Smith, A. (2008). The ground state of embryonic stem cell self-renewal.
542 Nature 453(7194):519-23.
543 32. Lengerke, C., Schmitt, S., Bowman, T.V., Jang, II.H., Maouche-Chretien, L.,
544 McKinney-Freeman, S., Davidson, A. J., Hammerschmidt, M., Rentzsch, F., Green,
545 J. B. A., et al. (2008). BMP and Wnt specify hematopoietic fate by activation of the
546 Cdx-Hox pathway. Cell Stem Cell 2(1):72-82.
547 33. Woods, N.B., Parker, A.S., Moraghebi, R., Lutz, M. K., Firth, A. L., Brennand, K. J.,
548 Berggren, W. T., Raya, A., Belmonte, J. C. I., Gage, F. H., et al. (2011). Brief report:
549 efficient generation of hematopoietic precursors and progenitors from human
550 pluripotent stem cell lines., Stem Cells (7):1158-64.
551 34. Gori, J. L., Chandrasekaran, D., Kowalski, J. P, Adair, J. E., Beard, B. C., D'Souza,
552 S. L., and Kiem, H-P. (2012). Efficient generation, purification, and expansion of
553 CD34(+) hematopoietic progenitor cells from nonhuman primate-induced pluripotent
554 stem cells. Blood 120(13):e35-44.
555 35. Garneau, N.L., Wilusz, J., and Wilusz, C.J. (2007). The highways and byways of
556 mRNA decay. Nat. Rev. Mol. Cell Biol. 8:113–126.
557 36. Lykke-Andersen, S., and Jensen, T.H. (2015) Nonsense-mediated mRNA decay: an
558 intricate machinery that shapes transcriptomes. Nat. Rev. Mol. Cell Biol. 16:665–677.

559 37. Débora M, P., Juliette, F., Mathieu, R., Anthony K, M., Aude, B., Martha, M.,
560 Michaela, M-T., Anne-Sophie, B., Frank, K., Sébastien, N., et al. (2016). Endogenous
561 TRIM5α Function Is Regulated by SUMOylation and Nuclear Sequestration for
562 Efficient Innate Sensing in Dendritic Cells. Cell Rep14(2):355-69
563 38. Taya, K., Nakayama, E. E., and Shioda, T. (2014). Moderate Restriction of
564 Macrophage-Tropic Human Immunodeficiency Virus Type 1 by SAMHD1 in
565 Monocyte-Derived Macrophages. PLoS One 9(3):e90969.
566 39. Abed, S., Tubsuwan, A., Chaichompoo, P., Park, I. H., Pailleret, A., Benyoucef, A.,
567 Tosca, L., De Dreuzy, E., Paulard, A., Granger-Locatelli, M., et al. (2015).
568 Transplantation of Macaca cynomolgus iPS-derived hematopoietic cells in NSG
569 immunodeficient mice. Haematologica. 100: e428-e431
570 40. Katayama, M., Hirayama, T., Horie, K., Kiyono, T., Donai, K., Takeda, S., Nishimori,
571 K., and Fukuda, T. (2016). Induced pluripotent stem cells with six reprogramming
572 factors from Prairie Vole, which is an animal model for social behaviors. Cell
573 Transplantation.
574 41. Katayama, M., Hirayama, T., Tani, T., Nishimori, K., Onuma, M., and Fukuda, T.
575 2018. Chick derived induced pluripotent stem cells by the poly-cistronic transposon
576 with enhanced transcriptional activity. Journal of Cellular Physiology, 233:990-1004.

Figure Legends

Figure1. Generation of Rh-iPSCs from Rh PBMCs

(a) Schematic illustration showing the reprogramming of PBMCs to Rh-iPSCs. (b) Phase contrast images of iPSC colonies from 3 individuals. Scale bars, 200 μm. (c) Summary of the Rh-iPSC generation. (d) RT-PCR analysis of SeV vectors. GAPDH was examined as an internal control. (e) RT-PCR analysis of pluripotency-associated genes. GAPDH was examined as an internal control. (f) Flow-cytometric analysis of SSEA-4 expression. (g)Teratoma formation assay shows derivatives of all three germ layers. GE: gut-like epithelium, C: cartilage, M: muscle tissue, NC: neural crest, ML: melanocytes. Scale bars, 50 μm (h) Chromosomal analysis of Rh-iPSCs.

Figure2. Differentiation of Rh-iPSCs into HPCs

(a) Schematic illustration showing Rh-iPSC differentiation to HPCs. (b) Phase contrast images of Sac differentiation on days 0, 4, 8, and 14. Scale bars, 200 μm. (c) Flow-cytometric analysis of the HPC phenotypes 14 days after starting the differentiation. Upper panels, unstained cells; lower panels, stained cells. (d) Dot plots show the

593 differentiation efficiency into CD34(+) cells of 3 Rh-iPSC clones with or without
594 BMP4. *p < 0.05; **p <0.01. (e) A bar graph displaying the number of colony-forming
595 units. Data are plotted as the mean ± SD of triplicate samples. The microscopic images
596 show colony morphology (upper panels) and cytospins (lower panels). G, granulocytes;
597 M, macrophages; GM, granulocytes/macrophages; E, erythroid. Scale bars, 100 μm
598 (top) and 50 μm (bottom).

599

600 **Figure3. Differentiation of Rh-iPSCs into macrophages**

601 (a) Schematic illustration of the differentiation into macrophages from HPCs. Phase
602 contrast images of macrophage differentiation on days 24 and 34 (left, middle) and
603 cytospins on day 34 (right). Scale bars, 50 μm. (b) Flow-cytometric analysis of the
604 macrophage phenotypes 34 days after the differentiation. (c) Macrophages were
605 incubated with Alexa Flour594 Escherichia coli and observed 1 hour later. Microscopic
606 images show bioparticles localized in the macrophages. Scale bars, 100 μm. (d)
607 Cytokine production by macrophages differentiated from Rh-iPSCs. Data are plotted as
608 the mean ± SD of triplicate samples. **** p <0.0001. (e) Detection of SIVmac316 in
609 iPSC-derived macrophages by ELISA. HSC-F is a cynomolgus monkey T-cell line and

610 control. Replication was monitored by determining the amount of p27 in the culture
611 supernatant at days 1, 4, and 7 after the incubation. Data are plotted as the mean ± SD of
612 triplicate samples. * $p < 0.05$, **** $p < 0.0001$ for comparisons between SIV mac 316
613 and SIV mac 239. :iMac, iPSC-derived macrophages.

614

615 **Figure4. Generation of TRIM5α-KO Rh-iPSCs**

616 (a) Schematic illustration of the sgRNA target site in the Rh *TRIM5* gene. (b) The
617 sgRNA target sequence and efficiency of the genome editing. (c) Sequence data of the
618 TRIM5**α** homo-KO iPSC clones and parental iPSC clone. Three established clones had
619 biallelic frameshift mutations in the *TRIM5* gene at the indicated sites. (d) Rh *TRIM5*
620 expression in TRIM5**α** homo-KO iPSC clones and parental iPSC clone was evaluated
621 with real-time PCR. Fold changes relative to primary Rh T cells are shown. (e) The
622 differentiation efficiency to CD34(+) cells of parental and TRIM5**α**-KO iPSCs. Three
623 independent experiments. (f) Flow-cytometric analysis of macrophage-marker
624 expression in macrophages generated from parental and TRIM5**α**-KO iPSCs.

625

Figure5. Deletion of TRIM5a enables HIV-1 virus infection

(a) Significant increase of HIV luminescence of TRIM5**α**-KO iMac compared to parental iMac. Macrophages (1×10^5 cells/well) were infected with NL43- Luci/VSV-G (10 ng of p24 virus) in a 24-well plate. Luciferase activity was measured 2, 3, and 4 days after the infection. Data are plotted as the mean ± SD of triplicate samples and presented as three independent measurements. * $p < 0.05$, *** $p < 0.001$, **** $p < 0.0001$ for comparisons between TRIM5**α**-KO iMac and parental iMac. (b) NL43-Luci/VSV-G infection was inhibited by Nevirapine (NVP). Macrophages (5×10^4 cells/well) were infected with NL43-Luci/VSV-G (6.6 ng of p24 virus) in a 96-well plate. Luciferase activity was measured 2 days after the infection. Data are plotted as the mean ± SD of triplicate samples and presented as three independent measurements of a single experiment. **** $p < 0.0001$ for comparisons between TRIM5**α**-KO iMac and parental iMac.

Table 1. Summary of CD34(+) cells from rh-iPSCs (confluent in 6-cm dish)

	Total cells (×10^6)	CD34 (+) %	CD34 (+) cells (×10^6)
R1863#7	8.69 ± 0.107	31.467 ± 5.147	2.63 ± 0.009
R1887#1	15.07 ± 0.30	25.567 ± 3.1	3.92 ± 0.110
R1889#3	18.91 ±0 .856	23.267 ± 6.716	3.48 ± 0.068

Data shown are mean ± SE from three independent experiments.

643

644

645

646

647

648

649

650

651

652

653

Table2. Results of off-target sequence analysis of top five off-target candidates determined by the CFD score of TRIM5 gRNA

	Position	Sequence	No. of mismatches	CFD off-target score	KO iPSC #1	KO iPSC #2	KO iPSC #3
TRIM5 on-target	chr14:67658119-110054350	CTACGACAAAACCAACGTCT CGG	-	1.0000	**-14 bp , -14 bp**	**-5 bp , -14 bp**	**-14 bp , -14 bp**
Potential off-target sites	chr4:103904324-103904346	CTATAATAAAACCAACATCT TGG	4	0.525778	WT	WT	WT
	chr2:76073316-76073338	CTAAGGCAAAAACAACATCT AGG	4	0.401003	WT	WT	WT
	chr2:98763243-98763265	CTGCCACAAACCCAACATCT TGG	4	0.179259	WT	WT	WT
	chr7:42594298-42594320	ATAAGATAAAACCAACGTCT GAG	3	0.177388	WT	WT	WT
	chr9:104127964-104127986	CTACAAAGAAACCAACTTCT AGG	4	0.119167	WT	WT	WT

Figure 1

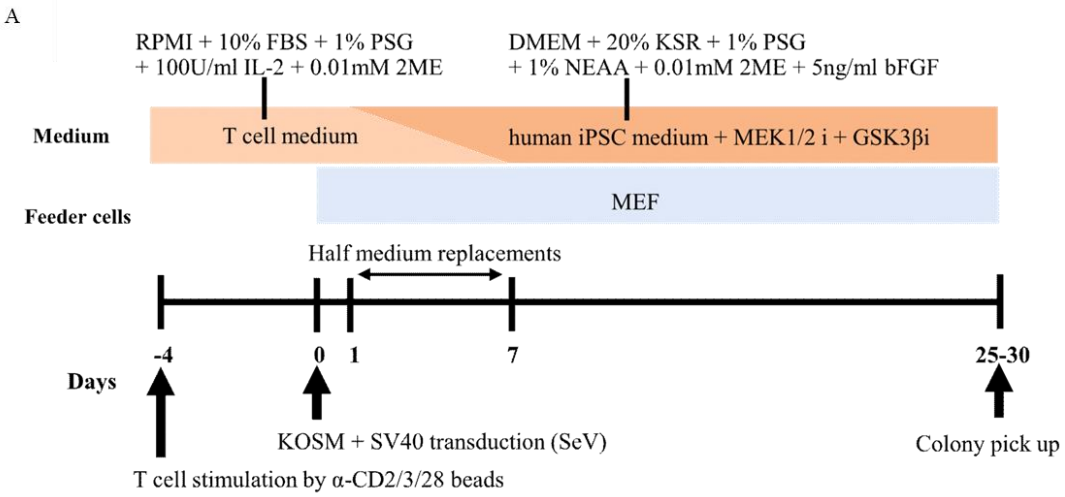

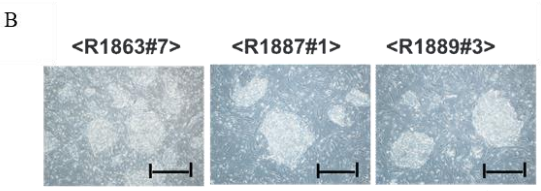

C

Animal ID	sex	Age at blood sampling	Input cell	Number of iPSC clones
R1863	male	6y2m	2×10^6 cells	3
R1887	male	6y1m	2×10^6 cells	2
R1889	male	6y1m	2×10^6 cells	4

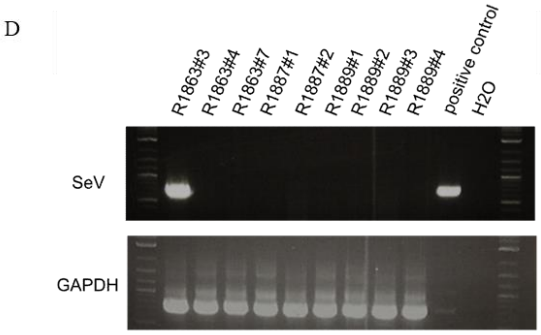

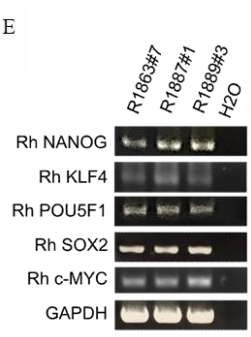

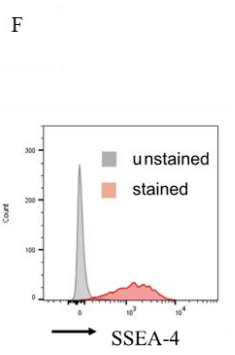

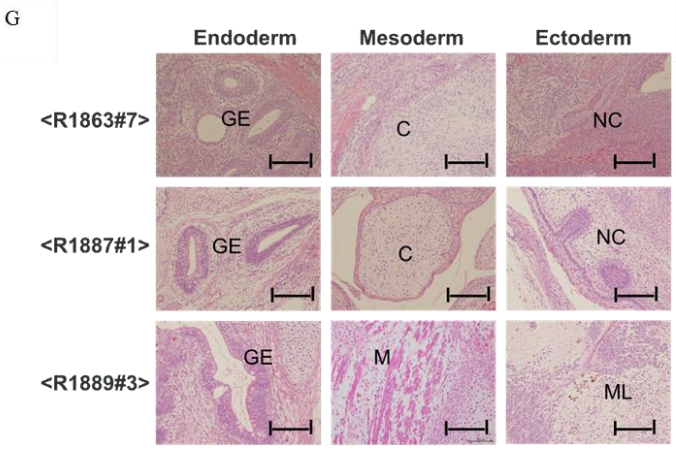

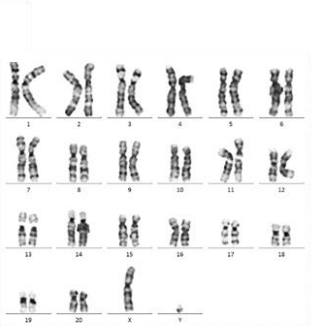

Figure 2

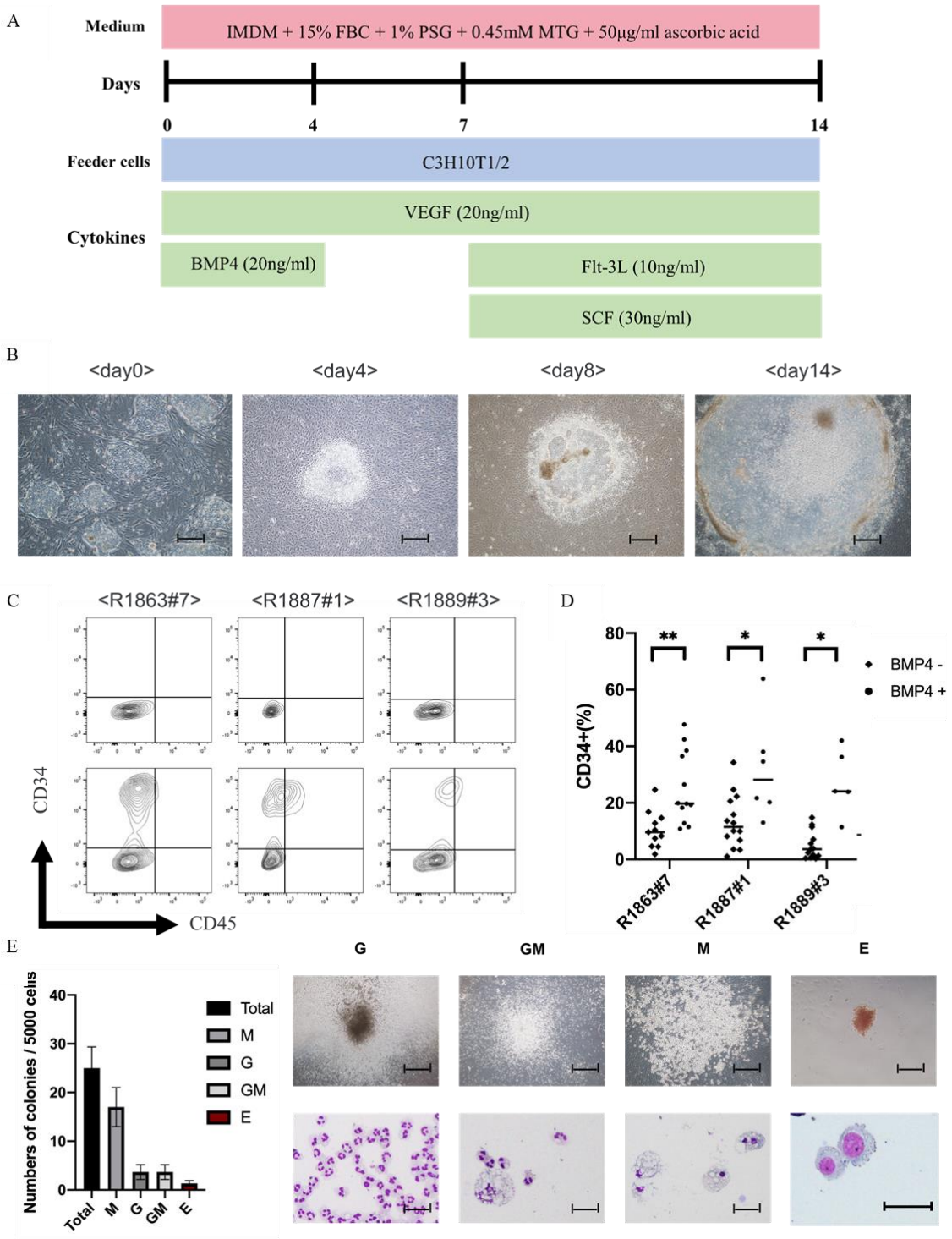

665

666

667

Figure 3

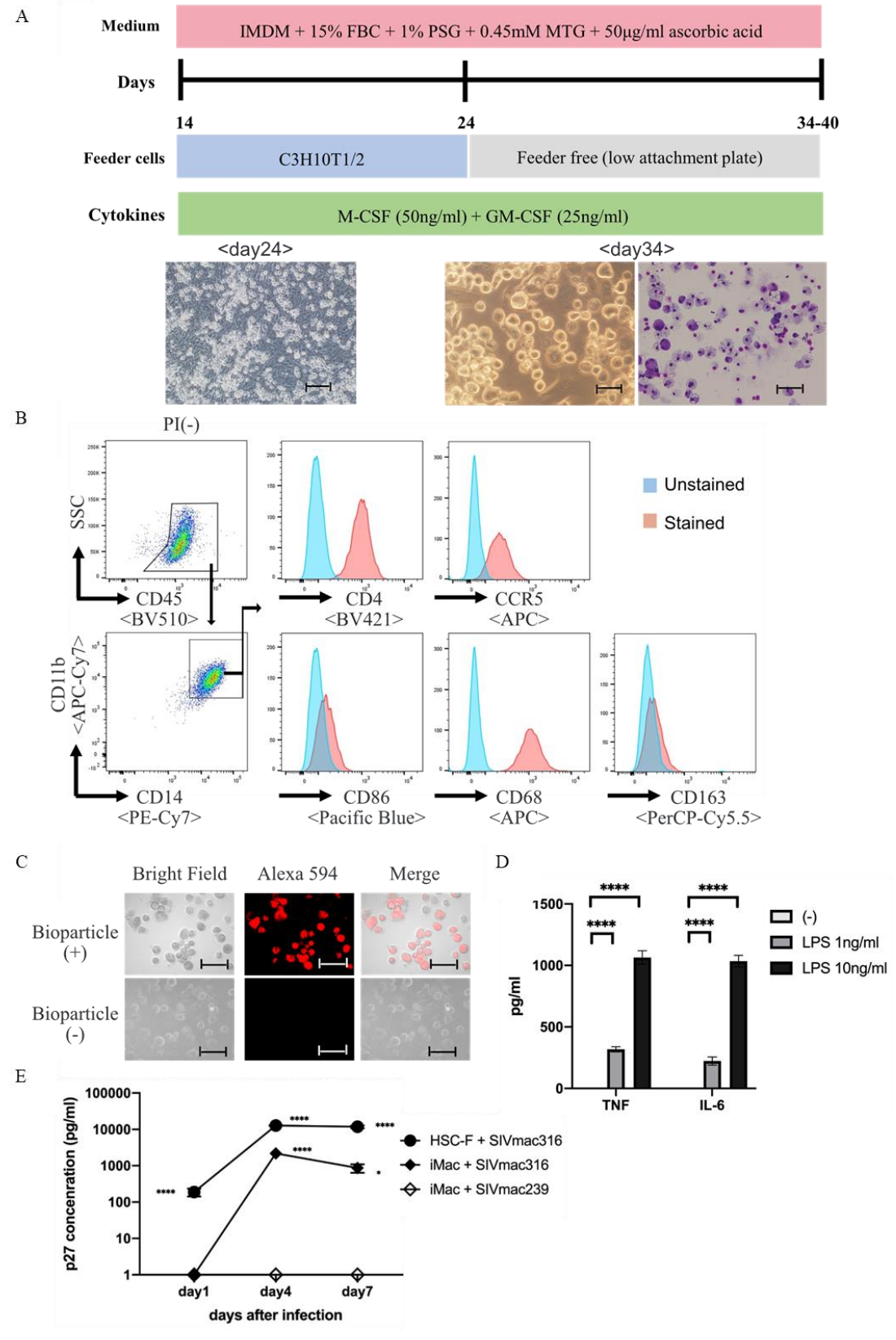

668

669

Figure 4

A

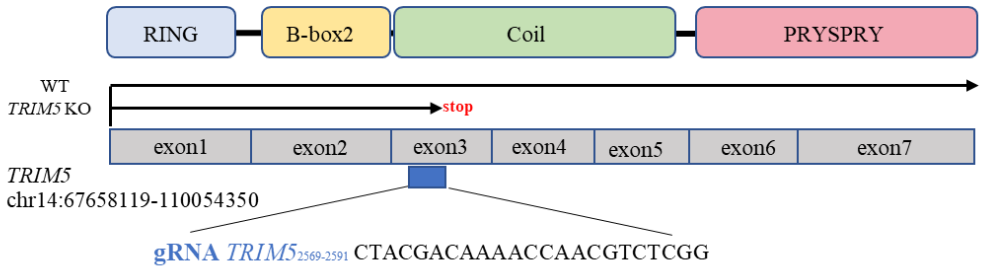

B

Target sequence	CTACGACAAAACCAACGTCTCGG
#(%) Total mutant clones	7(29.1)
#(%) Biallelic mutant clones among total mutant clones	3(42.8)

(total clone number : 24)

C

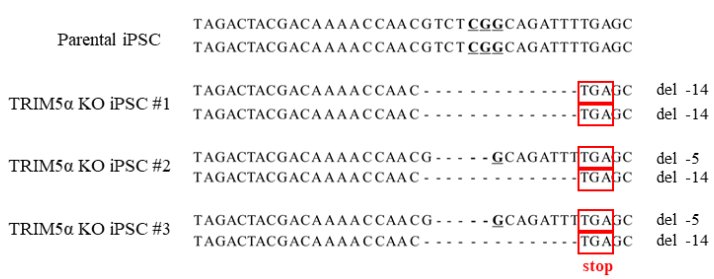

D

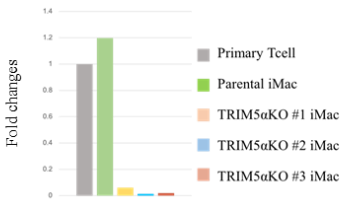

E

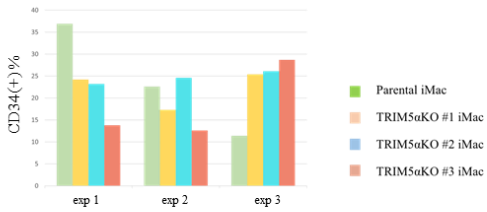

F

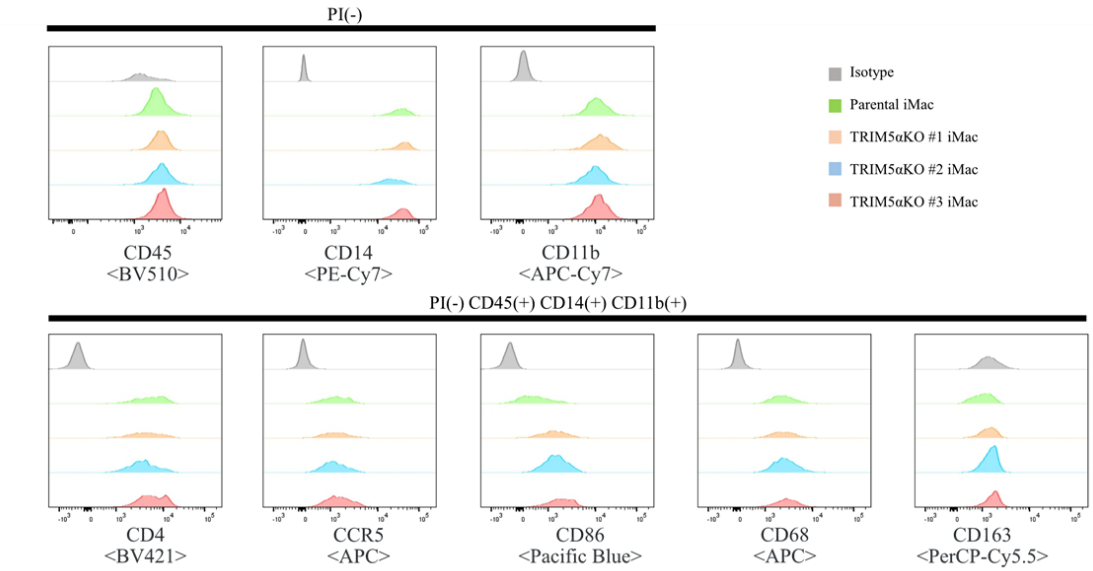

Figure 5

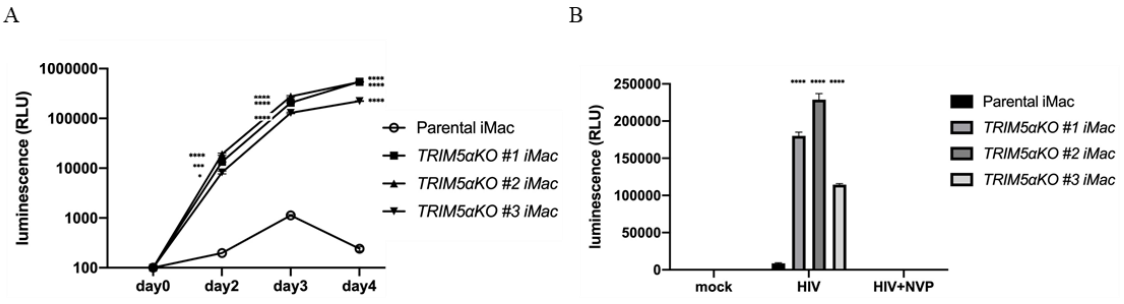
A
B
luminescence (RLU)
1000000
100000
10000
1000
100
day0
day2
day3
day4
Parental iMac
TRIM5αKO #1 iMac
TRIM5αKO #2 iMac
TRIM5αKO #3 iMac
250000
200000
150000
100000
50000
0
mock
HIV
HIV+NVP

Figure S1

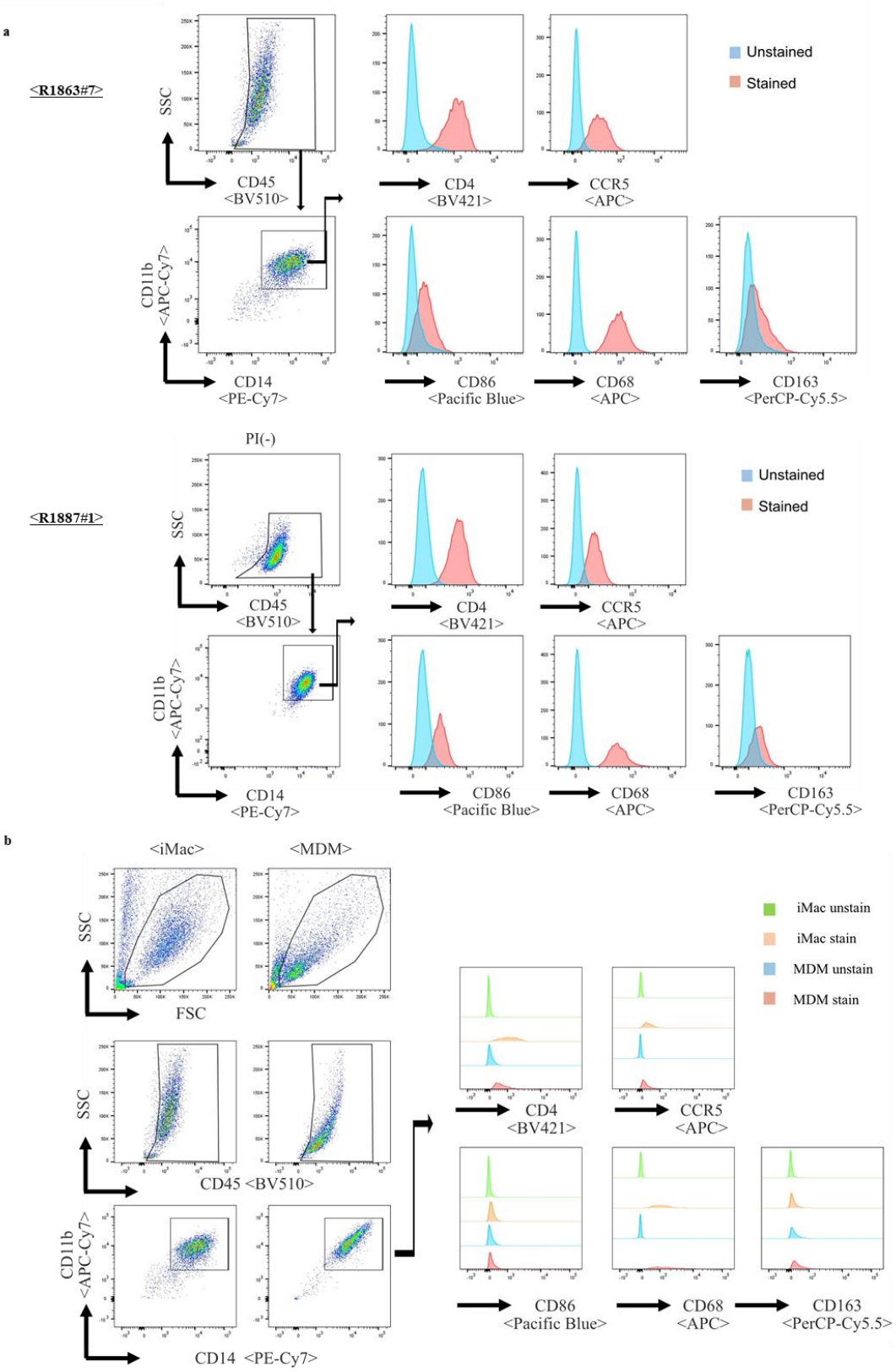

687

Figure S1 Flow-cytometric analysis of the macrophage differentiated from Rh-iPSC

(a)Flow-cytometric analysis of the macrophage generated from other Rh-iPSC clones phenotypes 34 days after the differentiation.

(b)Flow-cytometric analysis of macrophage-marker expression in macrophages generated from Rh-iPSCs and monocytes (MDM).

706 **Table S1**

707 Results of CRISPR/Cas9 genome editing by using Cas9 and gRNA expression plasmid (Exp1,2) or

708 Cas9 protein and sgRNA (Exp3,4)

709

	Efficacy of genome editing
Exp1: Cas9 and gRNA expression plasmid	0%
Exp2: Cas9 and gRNA expression plasmid	0%
Exp3: Cas9 protein and sgRNA	29.1%
Exp4: Cas9 protein and sgRNA	40%

710

711